Department of Physics and Astronomy
University of Heidelberg

Bachelor Thesis in Physics
submitted by

Linda Shen

born in Greven (Germany)

2015

LHC Phenomenology of $Z^{'} \to e^{+}e^{-}$ decays in the $(B-L)$SSM

This Bachelor Thesis has been carried out by Linda Shen at the
Institute for Theoretical Physics in Heidelberg
under the supervision of Prof. Tilman Plehn

Abstract

The search for possible sneutrino-antisneutrino oscillations lead to a viable point in the the parameter space of the $(B-L)$SSM extension of the MSSM. For this parameter set $Z' \to e^+e^-$ events in proton-proton collisions at a center-of-mass energy of 13 TeV are analysed. By extrapolation to higher masses a Z' resonance could be excluded at 95 % confidence level for masses less than 3.2 TeV for a luminosity of $20\,\mathrm{fb}^{-1}$, 3.9 TeV for $100\,\mathrm{fb}^{-1}$, and 5.4 TeV for $3000\,\mathrm{fb}^{-1}$ in the dielectron channel.

Zusammenfassung

Die Suche nach Sneutrino-Antisneutrino-Oszillationen im $(B-L)$SSM führte zu einem Set von Parametern, für welche nun der Z' Zerfall in Elektron-Positron-Paare untersucht wird. Dazu werden Protonen betrachtet, die bei einer Schwerpunktsenergie von 13 TeV kollidieren. Mit einer Sicherheitswahrscheinlichkeit von 95 % konnte eine Z' Resonanz unter 3.2 TeV für eine Luminisität von $20\,\mathrm{fb}^{-1}$, unter 3.9 TeV für $100\,\mathrm{fb}^{-1}$ und unter 5.4 TeV für $3000\,\mathrm{fb}^{-1}$ ausgeschlossen werden.

Contents

1 Introduction

The Standard Model (SM), describing fundamental particles and their interactions, has become a well-tested physics theory. Within its domain the SM successfully explains and precisely predicts a wide variety of experimental results. However, there are phenomena which cannot be explained by the Standard Model. It neither includes a quantum theory of gravity nor dark matter. For instance, according to cosmology only a small fraction of the universe's total energy is made up by SM particles. Also the SM does not provide enough CP violation to explain the baryonic matter-antimatter asymmetry of the universe. Further, the hierarchy problem and experimentally observed neutrino oscillations cannot be explained in the SM where neutrinos are massless [8, 19].

Supersymmetry (SUSY) is an approach that unifies the gauge couplings, solves the hierarchy problem, provides a candidate for dark matter and explains electroweak symmetry breaking (EWSB). However, there is no evidence for SUSY yet. In addition, there are still problems that SUSY cannot address such as neutrino masses, the strong CP problem and the μ problem. Therefore, the relevance of exploring non-minimal SUSY extensions is rising. In this work we will introduce the $(B-L)$ Supersymmetric Standard Model (BLSSM) that contains an additional $U(1)_{B-L}$ gauge group. It uses right-handed sneutrino fields to provide a solution for the existence and smallness of left-handed neutrino masses and also includes a dark matter candidate. With the availability of higher energies in experiments, e.g. at the Large Hadron Collider (LHC), the production of new particles and thus evidence for an extension of the SM is expected [19].

The impetus for this project is the paper "Right-handed sneutrino-antisneutrino oscillations in a TeV scale supersymmetric $B-L$ model" by Elsayed et al. [15]. Therein they discussed prospects of examining SUSY partners of the right-handed neutrino in the BLSSM. Elsayed et al. proposed two decay chains that could probe sneutrino oscillations. The motivation for these channels is their non-vanishing signals in a detector. While the paper assumed that a pure sample of sufficient size of these chains could be extracted from the LHC data, it proved difficult to find a valid point in the parameter space of the BLSSM that would allow such events.

One of the decay chains examined by Elsayed et al. contains a Z' as an intermediate state. The Z' is a boson arising from the additional symmetry group in the BLSSM. As the ATLAS detector at the LHC searches for high-mass resonances decaying to dielectron or dimuon final states, it is interesting to study these decays for the Z' in the BLSSM. In this Bachelor thesis $Z' \to e^+e^-$ processes will be analysed for a parameter set originally aimed on sneutrino oscillation phenomenology. Further, we will calculate exclusion limits for the Z' mass and thus restrict the BLSSM.

The work is organized as follows: An overview over the SM and the MSSM is given in Section 2 followed by an outline of the BLSSM in Section 3. Therein, the common parameters of the MSSM and the BLSSM are presented since in Section 4

the parameter space of the BLSSM is considered without universal soft supersymmetry breaking terms. Then we will present the analysis of Z' to dielectron decays in Section 5 where we introduce the CL_s method to calculate exclusion limits on the Z' mass. Finally, we will briefly summarize and give an outlook.

2 Theoretical Background

In this section we will first consider the SM and then go over to the MSSM as an extension of the SM that realizes supersymmetry.

In particle physics, quantum mechanical models of subatomic particles are constructed with a quantum field theory, i.e. a field characterized by quantum operators. Particles are then treated as excited states of an underlying physical field. The SM describes electromagnetic, weak and strong interaction by quantum gauge theories. Gauge theories are field theories, in which the Lagrangian is invariant under a continuous group of local transformations. These gauge transformations form a Lie group which is referred to as the symmetry group or the gauge group of the theory. Associated with the group is the Lie algebra of group generators whereby each group generator corresponds to a gauge field with quantum states, so-called gauge bosons.

2.1 The Standard Model and its Symmetry Groups

The SM includes 17 fundamental particles which can be divided into fermions and bosons. Fermions have half-integer spin and occur in two basic types called quarks and leptons, which are the building blocks of matter. Bosons have integer spin and two kinds exist in the SM. Gauge bosons have spin 1 and are responsible for mediating forces whilst the Higgs boson has spin 0 and gives mass to the fundamental particles. The elementary particles of the SM are shown in Figure 1. The fermions occur in three generations with two types each.

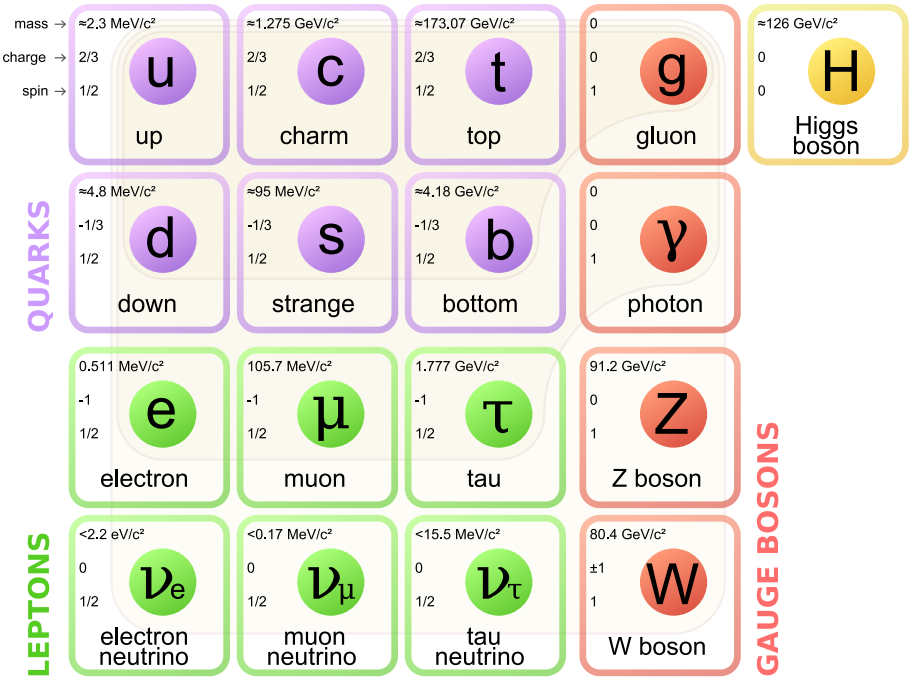

Figure 1: Elementary particles of the SM. Image taken from [14].

The SM describes three (of the four) known forces, each mediated by gauge bosons as force carrier: electromagnetism by photons, the weak force by $W^{\pm}$ and Z bosons, and the strong force by gluons. Not included is the gravitational force. With these forces interactions between the different groups of particles can be described. The strength of a force is given by the so-called coupling constant, a dimensionless number determined by the charge of a force. The fine structure constant

$$\alpha_e = \frac{e^2}{4\pi\hbar c} \approx \frac{1}{137} \tag{2.1}$$

provides a measure for the electromagnetic force. In analogy, colour charge determines a coupling constant α_s for the strong force and weak charge a coupling constant α_W for the weak force. The strong coupling has magnitude of order 1 for hadrons and decreases at smaller distances, whereas the weak coupling is in the order of $1/30$ [18]. If we consider colour charge and include antiparticles, there are 61 particles in total as demonstrated in Table 1.

	Types	Generations	Antiparticle	Colours	Total
Quarks	2	3	Pair	3	36
Leptons	2	3	Pair	0	12
Gluons	1	1	Own	8	8
W boson	1	1	Pair	0	2
Z boson	1	1	Own	0	1
Photon	1	1	Own	0	1
Higgs	1	1	Own	0	1
					61

Table 1: Full particle content of the SM

The gauge group of the SM is

$$SU(3)_C \times SU(2)_L \times U(1)_Y \tag{2.2}$$

Here $SU(3)_C$ represents the strong force since gluons are gauge bosons of the symmetry group $SU(3)$ and carry color charge indicated by the index C. The gauge structure $SU(2)_L \times U(1)_Y$ unifies electromagnetic interactions and weak interactions where the Y stands for the weak hypercharge. The reason for the index L is that left-handed fermions transform under both $SU(2)_L$ and $U(1)_Y$, whereas right-handed fermions only transform under $U(1)_Y$. Due to massless neutrinos in the SM there is no right-handed state of the neutrino. Hence, leptons appear as shown in Table 2.

In the unbroken electroweak theory the gauge fields are an isotriplet of W_μ for $SU(2)_L$ and a singlet B_μ for $U(1)_Y$ which lead to the massless gauge bosons W^+, W^-, W^0 and B^0. However, interactions with the Higgs field give rise to spontaneous symmetry breaking, also called electroweak symmetry breaking (EWSB). As

weak isospin doublets	weak isospin singlets
$\begin{pmatrix}\nu_e\\ e\end{pmatrix}_L \begin{pmatrix}\nu_\mu\\ \mu\end{pmatrix}_L \begin{pmatrix}\nu_\tau\\ \tau\end{pmatrix}_L$	e_R, μ_R, τ_R
$\begin{pmatrix}\bar{e}\\ \bar{\nu}_e\end{pmatrix}_R \begin{pmatrix}\bar{\mu}\\ \bar{\nu}_\mu\end{pmatrix}_R \begin{pmatrix}\bar{\tau}\\ \bar{\nu}_\tau\end{pmatrix}_R$	$\bar{e}_L, \bar{\mu}_L, \bar{\tau}_L$

Table 2: Lepton sector in the SM

a consequence, gauge and fermion fields obtain masses and a new neutral scalar particle appears, the Higgs boson. Mixing of the W^0 and the B^0 result in the massless gauge boson γ and the massive gauge boson Z. Altogether, we get one massless gauge boson γ, three massive gauge bosons W^+, W^-, Z and the Higgs boson H.

EWSB further leads to mixing of quark flavours, also known as generation mixing. Here, the weak eigenstates become linear superpositions of the mass eigenstates. With d'_L, s'_L, b'_L being combinations of d_L, s_L, b_L, the states can be written as displayed in Table 3.

weak isospin doublets	weak isospin singlets
$\begin{pmatrix}u\\ d'\end{pmatrix}_L, \begin{pmatrix}c\\ s'\end{pmatrix}_L, \begin{pmatrix}t\\ b'\end{pmatrix}_L$	$u_R, c_R, d_R;\ t_R, s_R, b_R$
$\begin{pmatrix}\bar{d}\\ \bar{u}'\end{pmatrix}_R, \begin{pmatrix}\bar{s}\\ \bar{c}'\end{pmatrix}_R, \begin{pmatrix}\bar{b}\\ \bar{t}'\end{pmatrix}_R$	$\bar{u}_L, \bar{c}_L, \bar{d}_L;\ \bar{t}_L, \bar{s}_L, \bar{b}_L$

Table 3: Quark sector in the SM

Because the SM does not include any ν_R fields, neutrinos cannot obtain mass and mixing among the three massless neutrino states has no meaning. If the neutrino is massless, there is no need to for right-handed neutrinos and left-handed antineutrinos [7].

2.2 Supersymmetry

The SM is completely successful for low-energy phenomena but a new framework will be necessary at the Planck scale ($\approx 10 \cdot 10^{19}\,\text{GeV}$), where gravitational effects become important. Also the SM does not explain the mass spectrum, the reason for three generations or the difference between the gauge couplings of strong and

electroweak forces. It is assumed that there is a higher symmetry from a very large mass scale M_χ onwards. One idea is that above M_χ all gauge couplings become the same coupling α_G, while below M_χ spontaneous symmetry breaking results in separate couplings α_i for the different groups. The Grand Unification Theory (GUT) poses the idea that $SU(3)$, $SU(2)$ and $U(1)$ are subgroups of a larger symmetry group G where quarks and leptons belong to the same multiplets. Attempts for a realistic GUT include proposals such as $G = SU(5)$ and $G = SU(10)$. Unlike in the SM, in supersymmetric models the gauge couplings can unify. Therefore, SUSY might be a hint for a GUT [7, 22].

SUSY is an attempt to unify the treatment of particles with different spins. Consequently, fermions and bosons are related to each other. Every fundamental particle is associated with a so-called superpartner having similar properties but a spin differing by 1/2. The partners are called *sparticles* and their names are shown in Table 4. For fermions a prefix "s-" and for bosons a suffix "-ino" is added to the original name. Due to symmetry breaking the photino, zino, winos and Higgsinos are not mass eigenstates [7].

Particle		Spin	Sparticle		Spin
quark	q_L, q_R	$\frac{1}{2}$	squark	$\tilde{q}_L, \tilde{q}_R$	0
lepton	ℓ_L, ℓ_R	$\frac{1}{2}$	slepton	$\tilde{\ell}_L, \tilde{\ell}_R$	0
photon	γ	1	photino	$\tilde{\gamma}$	$\frac{1}{2}$
gluon	g	1	gluino	$\tilde{g}$	$\frac{1}{2}$
W boson	W	1	wino	$\tilde{W}$	$\frac{1}{2}$
Z boson	Z	1	zino	$\tilde{Z}$	$\frac{1}{2}$
Higgs	H	0	Higgsino	$\tilde{H}$	$\frac{1}{2}$

Table 4: Supersymmetric particles

2.2.1 Mass Spectrum of the MSSM

The simplest extension of the SM that realizes supersymmetry is the Minimal Supersymmetric Standard Model (MSSM). It can unify the gauge couplings, solve the hierarchy problem, provide a candidate for dark matter and explain electroweak symmetry breaking (EWSB). However, there are still aspects the MSSM cannot address such as neutrino masses, the strong CP problem, and the μ problem.

Table 5 and Table 6 show the fundamental particles of the MSSM. For quarks and leptons only the first generation is displayed. In Table 5 chiral supermultiplets are labelled by their superfields. It is a standard convention to define all chiral supermultiplets by left-handed fields. The multiplets of the right-handed fermions are described by their charge conjugates, indicated by the superscript c. Capital letters indicate $SU(2)_L$-doublet chiral supermultiplets while small letters stand for $SU(2)_L$-singlet chiral supermultiplets [22].

	Particle	Spin $\frac{1}{2}$	Sparticle	Spin 0	$SU(3)_C$	$SU(2)_L$	$U(1)_Y$
$\hat{Q}$		(u_L, d_L)		$(\tilde{u}_L, \tilde{d}_L)$	**3**	**2**	$\frac{1}{6}$
$\hat{u}^c$	quarks	u^c	squarks	$\tilde{u}^c$	$\bar{\mathbf{3}}$	**1**	$-\frac{2}{3}$
$\hat{d}^c$		d^c		$\tilde{d}^c$	$\bar{\mathbf{3}}$	**1**	$\frac{1}{3}$
$\hat{L}$	leptons	(ν_e, e_L)	sleptons	$(\tilde{\nu}_e, \tilde{e}_L)$	**1**	**2**	$-\frac{1}{2}$
$\hat{e}^c$		e^c		$\tilde{e}^c$	**1**	**1**	1
$\hat{H}_u$	Higgs	$(\tilde{H}_u^+, \tilde{H}_u^0)$	Higgsinos	(H_u^+, H_u^0)	**1**	**2**	$\frac{1}{2}$
$\hat{H}_d$		$(\tilde{H}_d^0, \tilde{H}_d^-)$		(H_d^0, H_d^-)	**1**	**2**	$-\frac{1}{2}$

Table 5: Chiral supermultiplets of the MSSM

Particle	Spin 1	Sparticle	Spin $\frac{1}{2}$	$SU(3)_C$	$SU(2)_L$	$U(1)_Y$
gluon	g	gluino	$\tilde{g}$	**8**	**1**	0
W bosons	$W^\pm, W^0$	winos	$\tilde{W}^\pm, \tilde{W}^0$	**1**	**3**	0
B boson	B^0	bino	$\tilde{B}^0$	**1**	**1**	0

Table 6: Gauge supermultiplets of the MSSM

2.2.2 R-parity

R-parity is a symmetry introduced to distinguish SM particles and their superpartners. Some supersymmetric Lagrangians are invariant under transformations of a global $U(1)_R$ symmetry, which act differently on the component fields of the superfields. If the phase, which parametrizes the R transformations, is restricted to π, supersymmetry generators can either have R charge $+1$ or -1. This is often referred to as R-parity. SM particles have $R = 1$ while their superpartners have $R = -1$ [19].

R-parity can be calculated with baryon number B, lepton quantum number L and spin s:

$$R = (-1)^{3(B-L)+2s} \tag{2.3}$$

Under conservation of R-parity sparticles are always produced in pairs and they decay, either directly or in a R-conserving cascade process, into a stable sparticle, the lightest supersymmetric particle (LSP). Hence, the Universe must be filled with LSPs. From cosmology we know that dark matter particles need to carry no electric or color charge. If the LSP is neutral in this sense, it seems to be a viable candidate for dark matter [22].

The MSSM is defined to conserve R-parity. This decision is motivated phenomenologically by proton decay constraints and the hope that the LSP provides a good candidate for dark matter. However, it is also possible that R-parity is broken

or replaced by some other symmetry [22].

2.2.3 EWSB in the MSSM

As EWSB causes mixing of the Higgs and the gauge bosons in the SM, it also leads to mixing of the Higgs bosons and the Higgsinos with the electroweak gauginos.

After EWSB, the complex Higgs doublets (H_u^+, H_u^0) and (H_d^0, H_d^-) form the longitudinal modes of the W^+, W^-, Z vector bosons and the five mass eigenstates h^0, H^0, A^0, H^+, H^-. The neutral Higgsinos $\tilde{H}_u^0$, $\tilde{H}_d^0$ and the neutral gauginos $\tilde{B}^0$, $\tilde{W}^0$ combine to four mass eigenstates called neutralinos: χ_i^0 with $i = 1, 2, 3, 4$. The charged Higgsinos $\tilde{H}_u^+$, $\tilde{H}_d^-$ and the winos $\tilde{W}^+$, $\tilde{W}^-$ mix to two charged mass eigenstates called charginos: $\chi_i^\pm$ with $i = 1, 2$. By convention, these particles are labelled in ascending order of their masses:

$$m_{\chi_1^0} < m_{\chi_2^0} < m_{\chi_3^0} < m_{\chi_4^0}$$
$$m_{\chi_1^\pm} < m_{\chi_2^\pm}$$

Neutralinos and charginos all have spin 1/2. Since the lightest neutralino χ_1^0 is the LSP for a wide range of parameter space, it is a strongly favoured candidate for dark matter in the MSSM [22].

2.2.4 SUSY Breaking

If SUSY were an exact symmetry of nature, sparticles would have the same mass as their SM partners and should have been detected in experiments which is not the case. Hence, SUSY must be a broken theory and the superpartners must have larger masses than observable so far. Many mechanisms have been explored to explain how MSSM superpartners obtain their mass. Two of the most popular ones are

1. Gravity Mediated SUSY Breaking (SUGRA), where gravity acts as the messenger for SUSY breaking, and
2. Gauge Mediated SUSY Breaking (GMSB), where the transmission interaction is the same gauge interaction of the SM.

Both of these theories assume the existence of a hidden sector, which is responsible for the symmetry breaking, and an interaction transmitting the breaking to the visible sector [19].

Soft SUSY Breaking is a attempt to explain the mass differences between particles and their superpartners while preserving the coupling structure of the MSSM. This is parametrized by the following Lagrangian

$$\mathcal{L}_{\text{MSSM}}^{\text{soft}} = -\frac{1}{2}\left(M_1\tilde{B}\tilde{B} + M_2\tilde{W}\tilde{W} + M_3\tilde{g}\tilde{g} + \text{h.c.}\right) \tag{2.4}$$
$$-\left(\tilde{u}^c T_u \tilde{Q} H_u - \tilde{d}^c T_d \tilde{Q} H_d - \tilde{e}^c T_e \tilde{L} H_d + \text{h.c.}\right) \tag{2.5}$$
$$- m_{H_u}^2 |H_u|^2 - m_{H_d}^2 |H_d|^2 - \mu B_\mu (H_u H_d + \text{h.c.}) \tag{2.6}$$
$$- \tilde{Q}^* \mathbf{m_Q^2} \tilde{Q} - \tilde{L}^* \mathbf{m_L^2} \tilde{L} - (\tilde{u}^c)^* \mathbf{m_{\bar{u}}^2} \tilde{u}^c - (\tilde{d}^c)^* \mathbf{m_{\bar{d}}^2} \tilde{d}^c - (\tilde{e}^c)^* \mathbf{m_{\bar{e}}^2} \tilde{e}^c \tag{2.7}$$

M_1, M_2 and M_3 are the bino, wino and gluino bare mass terms. The scalar couplings T_u, T_d, T_e are complex 3×3 matrices corresponding to Yukawa couplings, whereas $\mathbf{m_Q^2}, \mathbf{m_L^2}, \mathbf{m_{\bar{u}}^2}, \mathbf{m_{\bar{d}}^2}, \mathbf{m_{\bar{e}}^2}$ are hermitian 3×3 matrices. $m_{H_u}^2$, $m_{H_d}^2$ and μB_μ are scalar squared-mass terms, where $m_{H_u}^2$ and $m_{H_d}^2$ are real while the Higgs mass squared-mass term is expressed in terms of the complex parameter B_μ and the higgsino mass parameter μ [13].

This Lagrangian introduces in total 105 new parameters compared to the SM. However, the hypothesis of soft supersymmetry breaking universality states that all mass matrices are proportional to the unit matrix and that the scalar couplings are proportional to their corresponding Yukawa matrix, i.e.

$$\mathbf{m_Q^2} = m_Q^2 \mathbb{1}, \quad \mathbf{m_L^2} = m_L^2 \mathbb{1}, \quad \mathbf{m_{\bar{u}}^2} = m_{\bar{u}}^2 \mathbb{1}, \quad \mathbf{m_{\bar{d}}^2} = m_{\bar{d}}^2 \mathbb{1}, \quad \mathbf{m_{\bar{e}}^2} = m_{\bar{e}}^2 \mathbb{1} \tag{2.8}$$

$$T_u = A_{u0} \mathbf{y_u}, \qquad T_d = A_{d0} \mathbf{y_d}, \qquad T_e = A_{e0} \mathbf{y_e}, \tag{2.9}$$

where the parameter A_{i0} is called trilinear coupling. Furthermore, in the minimal supergravity theory (mSUGRA) it is assumed that at GUT scale

1. soft-breaking scalar masses are universal

$$m_0^2 = m_{H_d}^2 = m_{H_u}^2 \tag{2.10}$$
$$m_0^2 = m_Q^2 = m_L^2 = m_{\bar{u}}^2 = m_{\bar{d}}^2 = m_{\bar{e}}^2 \tag{2.11}$$

2. gaugino masses are universal

$$M_{1/2} = M_1 = M_2 = M_3 \tag{2.12}$$

3. trilinear couplings are universal

$$A_0 = A_{u0} = A_{d0} = A_{e0} \tag{2.13}$$

This leads to five parameters: $M_{1/2}$, m_0^2, A_0, B_μ and μ. It is possible to express the parameters B_μ and μ via $\tan\beta$ and $|\mu|$, where the former is defined as the ratio of the Higgs vacuum expectation values (VEV):

$$\tan\beta \equiv \frac{\langle H_u^0 \rangle}{\langle H_d^0 \rangle} \tag{2.14}$$

Therefore, the MSSM mass spectrum in the mSUGRA model is determined by four unknown parameters and a sign:

$$M_{1/2},\ m_0^2,\ A_0,\ \tan\beta,\ \operatorname{sgn}\mu \tag{2.15}$$

This model is also refered to as constrained MSSM (CMSSM) [17, 19, 22, 23].

3 The $B-L$ Supersymmetric Standard Model

The BLSSM is a R-parity conserving extension of the MSSM where an extra $U(1)_{B-L}$ local gauge symmetry is postulated such that the full gauge group becomes

$$SU(3)_C \times SU(2)_L \times U(1)_Y \times U(1)_{B-L} \tag{3.1}$$

The invariance of the Lagrangian under this symmetry implies the existence of an additional gauge boson beyond the SM ones, the mass eigenstate Z', and an extra SM singlet scalar, the heavy Higgs. Besides, it is necessary to introduce three singlet fermion fields due to anomaly cancellation conditions. These fermions are called right-handed neutrinos ν_R.

The $B-L$ extension is motivated by two present observations: non-vanishing neutrino masses and the observed baryonic asymmetry in the universe, presumably due to CP violation. Both can be solved by introducing the right-handed neutrinos. Furthermore, the additional particles in this model lead to interesting signatures different from the SM results, which could be measured at the LHC [20].

3.1 Particle Content

Table 7 shows the particle content of the BLSSM. The superfield $\hat{\nu}^c$ represents the right-handed neutrinos. Moreover, two Higgs Superfields $\hat{\eta}$ and $\hat{\bar{\eta}}$, called bileptons, responsible for breaking the $B-L$ symmetry are added [15].

Superfield	Spin $\frac{1}{2}$	Spin 0	Gen.	$SU(3)_C$	$SU(2)_L$	$U(1)_Y$	$U(1)_{B-L}$
$\hat{Q}$	Q	$\tilde{Q}$	3	$\mathbf{3}$	$\mathbf{2}$	$\frac{1}{6}$	$\frac{1}{6}$
$\hat{u}^c$	u^c	$\tilde{u}^c$	3	$\bar{\mathbf{3}}$	$\mathbf{1}$	$-\frac{2}{3}$	$-\frac{1}{6}$
$\hat{d}^c$	d^c	$\tilde{d}^c$	3	$\bar{\mathbf{3}}$	$\mathbf{1}$	$\frac{1}{3}$	$-\frac{1}{6}$
$\hat{L}$	L	$\tilde{L}$	3	$\mathbf{1}$	$\mathbf{2}$	$-\frac{1}{2}$	$-\frac{1}{2}$
$\hat{e}^c$	e^c	$\tilde{e}^c$	3	$\mathbf{1}$	$\mathbf{1}$	1	$\frac{1}{2}$
$\hat{\nu}^c$	ν^c	$\tilde{\nu}^c$	3	$\mathbf{1}$	$\mathbf{1}$	0	$\frac{1}{2}$
$\hat{H}_u$	$\tilde{H}_u$	H_u	1	$\mathbf{1}$	$\mathbf{2}$	$\frac{1}{2}$	0
$\hat{H}_d$	$\tilde{H}_d$	H_d	1	$\mathbf{1}$	$\mathbf{2}$	$-\frac{1}{2}$	0
$\hat{\eta}$	$\tilde{\eta}$	η	1	$\mathbf{1}$	$\mathbf{1}$	0	-1
$\hat{\bar{\eta}}$	$\tilde{\bar{\eta}}$	$\bar{\eta}$	1	$\mathbf{1}$	$\mathbf{1}$	0	1

Table 7: Chiral superfields of the BLSSM

The extra gauge boson in the BLSSM is named B'. Analogous to EWSB, the bosons B, B' and W^0 mix to physical mass eigenstates γ, Z and Z'. Thus the extra gauge boson is known as Z' and is coupled to SM fermions by non-vanishing $B-L$ quantum numbers. Since the Z' could decay into a pair of leptons, there is

a promising channel for searching it at the LHC.

Further, due to the presence of two Abelian gauge groups, $U(1)_Y$ and $U(1)_{B-L}$, combined with the given particle content there is an additional effect called gauge kinetic mixing. It does not exist in the MSSM or other SUSY models with only one Abelian gauge group. One the one hand, gauge kinetic mixing leads to the mixing of the complex Higgs doublets with the bileptons $\eta, \bar{\eta}$. These four additional degrees of freedom from the bileptons become the longitudinal mode of the Z' and the mass eigenstates h', H', and A^0_η. One the other hand, a mixing of the MSSM neutralinos with the additional gauginos is induced, i.e. the mixing between $\tilde{H}^0_d, \tilde{H}^0_u, \tilde{B}^0, \tilde{W}^0, \tilde{B}', \tilde{\eta}, \tilde{\bar{\eta}}$. Thus, there are seven neutralinos in total now, refered to as χ^0_i with $i = 1, \ldots, 7$ [4, 21, 23].

3.2 SUSY Breaking and GUT Scale Boundary Conditions

With the extra particles in the BLSSM the soft SUSY Breaking terms of the Lagrangian are

$$\begin{aligned}\mathcal{L}^{\text{soft}}_{\text{BLSSM}} =& \mathcal{L}^{\text{soft}}_{\text{MSSM}} - \tilde{B}\tilde{B}' M_{BB'} - \frac{1}{2}\tilde{B}'\tilde{B}' M_{B'} - m^2_\eta |\eta|^2 - m^2_{\bar{\eta}} |\bar{\eta}|^2 \\ & - \mathbf{m^2_{\tilde{\nu}}}_{ij} (\tilde{\nu}^c_i)^* \tilde{\nu}^c_j - \eta\bar{\eta}\mu' B_{\mu'} + T^{ij}_\nu H_u \tilde{\nu}^c_i \tilde{L}_j + T^{ij}_x \eta \tilde{\nu}^c_i \tilde{\nu}^c_j \end{aligned} \tag{3.2}$$

where i, j are generation indices. B'_μ and B_μ can be chosen to be real and again mSUGRA motivated GUT scale boundary conditions can be assumed. For the new SUSY-breaking terms this means:

$$M_{B'} = M_{1/2} \tag{3.3}$$

$$\mathbf{m^2_{\tilde{\nu}}} = m^2_0 \mathbb{1} \qquad m^2_\eta = m^2_{\bar{\eta}} = m^2_0 \tag{3.4}$$

$$T_x = A_0 Y_x \qquad T_\nu = A_0 Y_\nu \tag{3.5}$$

At this scale off-diagonal terms are taken to be zero such that $M_{BB'}$ vanishes. Similar to the CMSSM, the parameters B_μ, $B_{\mu'}, \mu$ and μ' can be rephrased by $\tan\beta, \tan\beta', |\mu|$ and $|\mu'|$, where

$$\tan\beta' = \frac{\langle\eta\rangle}{\langle\bar{\eta}\rangle} \tag{3.6}$$

This leads to a free parameter set consisting of

$$M_{1/2},\ m^2_0,\ A_0,\ \tan\beta,\ \tan\beta',\ \operatorname{sgn}\mu,\ \operatorname{sgn}\mu',\ M_{Z'},\ Y_x,\ Y_\nu \tag{3.7}$$

Additional parameters to the MSSM are the mass of the Z' as well as the Yukawa matrices Y_x and Y_ν, where Y_ν has been constrained by neutrino data and must be very small compared to the other couplings in order to explain the light neutrino masses. Further, we can take Y_x diagonal since it is possible to choose a basis such that one of the Yukawa matrices is diagonal [21, 23].

3.3 Right-handed Sneutrino-antisneutrino Oscillation

In the slepton sector, the SUSY Breaking term $T_x^{ij}\eta\tilde{\nu}_i^c\tilde{\nu}_j^c$ in the Lagrangian leads to a splitting of the sneutrino states into real (scalar) and imaginary (pseudoscalar) parts. The result are 6 scalar states $\tilde{\nu}^S$ and 6 pseudoscalar states $\tilde{\nu}^P$. In general, the masses of scalar sneutrinos and pseudoscalar sneutrinos are different [21, 23].

While mixing between left- and right-handed sneutrinos is quite suppressed, between right-handed sneutrinos and right-handed antisneutrinos it seems plausible considering the associated Yukawa couplings. Whereas $\tilde{\nu}_L$ and $\tilde{\nu}_L^*$ are mass eigenstates, there is mass splitting and mixing between the right-handed sneutrino $\tilde{\nu}_R$ and antisneutrino $\tilde{\nu}_R^*$. The eigenvalues can be expressed as

$$m^2_{\tilde{\nu}_{R_{1,2}}} = m^2_{\tilde{\nu}_R} \pm \Delta m^2_{\tilde{\nu}_R} \tag{3.8}$$

where $m^2_{\tilde{\nu}_R}$ denotes the average heavy right-handed sneutrino squared mass given by

$$m^2_{\tilde{\nu}_R} = \frac{1}{2}(m^2_{\tilde{\nu}_{R_1}} + m^2_{\tilde{\nu}_{R_2}}) \tag{3.9}$$

and $\Delta m^2_{\tilde{\nu}_R}$ stands for the mass splitting between the sneutrinos. The eigenstates are then given by

$$\tilde{\nu}_{R_1} = \tilde{\nu}_R \cos\alpha + \tilde{\nu}_R^* \sin\alpha \qquad \tilde{\nu}_{R_2} = -i(\tilde{\nu}_R \sin\alpha - \tilde{\nu}_R^* \cos\alpha) \tag{3.10}$$

Here the mixing angle α depends on the sneutrino and antisneutrino mass difference $\Delta m^2_{\tilde{\nu}_R}$. For the right-handed (left-handed) sneutrinos the mass splitting is characterized by the size of the right-handed (left-handed) neutrino masses. Hence, the mass splitting of right-handed sneutrinos is large and we can take $\alpha = \frac{\pi}{4}$ to obtain the following mass eigenstates [15].

$$\tilde{\nu}_{R_1} = \frac{1}{\sqrt{2}}(\tilde{\nu}_R + \tilde{\nu}_R^*) \qquad \tilde{\nu}_{R_2} = \frac{-i}{\sqrt{2}}(\tilde{\nu}_R - \tilde{\nu}_R^*) \tag{3.11}$$

3.3.1 The Chargino Chain

While Elsayed et al. suggested two decay chains to analyse sneutrino oscillations in [15], here only the one containing a Z' is considered and will be refered to as chargino chain. It is shown in Figure 2. Requiring all intermediate states to be on mass-shell constrains the mass spectrum as follows:

$$M_{Z'} > M_{\tilde{\nu}_{R_{1,2}}} > M_{\tilde{\chi}_1^\pm} > M_{\tilde{\chi}_1^0} \tag{3.12}$$

In this decay mode a Z' is produced by a quark-antiquark-pair in a proton-proton-collision. Provided the aforementioned mass spectrum (3.12) it can decay into two right-handed sneutrinos ($\tilde{\nu}_{R_1}$ and $\tilde{\nu}_{R_2}$). These can then produce a lepton and a chargino. The latter can further decay into the lightest neutralino $\tilde{\chi}_1^0$, which

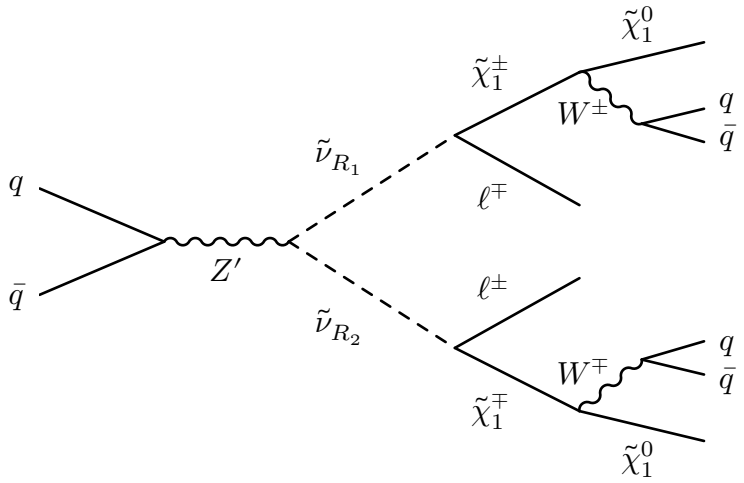

Figure 2: The chargino chain

we want to be the LSP, and a W boson that can decay hadronically.

Since conservation of helicity applies to strong, weak and electromagnetic interactions and holds in the relativistic limit, left-handed particles remain left-handed and right-handed particles remain right-handed in scattering processes at high energies [9].

The eigenstates $\tilde{\nu}_{R_1}$ and $\tilde{\nu}_{R_2}$ are composed of equal combinations of $\tilde{\nu}_R$ and $\tilde{\nu}_R^*$ as shown in (3.11) so they can decay into leptons or antileptons, i.e. into $\tilde{\chi}_1^+\ell^-$ or $\tilde{\chi}_1^-\ell^+$, with equal probability. Hence, the signal for the chargino chain consists of a same- or opposite-sign lepton pair plus two quark jets and missing energy for the LSPs. Signatures with same-sign leptons provide evidence for sneutrino-antisneutrino oscillation. If there was no oscillation, the Z' would decay into $\tilde{\nu}_R\tilde{\nu}_R^*$ which would only lead to opposite-sign lepton pairs [15].

4 Parameter Space

The parameter space of the BLSSM was explored in order to find a parameter set that can produce the chargino chain and is allowed by theory. For numerical calculations `SARAH` [28, 29, 30] version 3.3.1 and `SPheno` [25, 26] version 3.3.3 were used. The Mathematica package `SARAH` calculates vertices, mass matrices, renormalization group equations (RGEs), and loop corrections as well as the source code for `SPheno` for a given model. Then the mass spectrum and branching ratios of particle decays can be derived with `SPheno`. Event analysis was carried out with `MadGraph` and `CheckMATE` as will be presented in Section 5.

4.1 Expansion of the GUT Input Parameter Set

At first, we considered a scenario motivated by mSUGRA with the unknown parameters given in (3.7). However, this parameter set proved difficult for our purposes. Attempts to find a suitable energy spectrum for the chargino chain while respecting experimental constraints were not successful. The main problem with this set of parameters was that the sneutrino masses could not be made small enough without being in conflict with the Higgs boson mass $122\,\text{GeV} < M_h < 131\,\text{GeV}$ [2].

As a consequence, we expanded the mSUGRA inspired set of parameters by allowing more of the GUT scale breaking terms to vary independently. While the parameters A_0, $\tan\beta$, $\text{sgn}\,\mu$, $M_{Z'}$, $\tan\beta'$ and $\text{sgn}\,\mu'$ were kept, m_0 and $M_{1/2}$ are split into the parameters shown in Table 8. The expanded GUT input set then provided sufficient freedom to find viable points in the parameter space.

GUT scale parameter	new parameter
m_0	m_Q
	m_L
	m_{H_u}
	m_{H_d}
	$m_{\tilde{\nu}}$
	m_η
	$m_{\bar{\eta}}$
$M_{1/2}$	$M_1 = M_B$
	$M_2 = M_W$
	$M_3 = M_G$
	$M_{B'}$

Table 8: Expansion of the GUT parameters

4.2 Search of a Parameter Set for the Chargino Chain

First it was noticed that high values for the matrix elements of Y_x lead to small $m^2_{\tilde{\nu}}$ which would even become negative. A maximum acceptable value for degenerate Y_x

	ν_R	ν_L	$\chi_1^\pm$	χ_1^0	h
m_Q	⊗	⊗	○	○	⌀
m_L	⊗	⊗	○	○	⌀
m_{H_u}	⊗	⌀	○	○	○
m_{H_d}	⊗	○	○	○	○
$m_{\tilde{\nu}}$	⊗	⌀	○	○	○
m_B	⌀	⌀	⊗	⌀	○
m_W	⊗	⌀	⊗	⊗	○
m_G	○	○	⌀	⌀	⌀
$m_{B'}$	⊗	⊗	⌀	⌀	⊗
$\tan\beta$	○	⌀	⌀	○	⌀
$\tan\beta'$	⊗	⌀	○	○	○
A_0	⊗	○	⌀	⌀	⌀

Table 9: Relationships between expanded GUT parameters and masses of chargino chain spectrum. ⊗ describes sizeable, ⌀ small but noticeable, and ○ subtle influence.

matrix elements was found to be approximately 0.43. For the rest of the analysis we set the Yukawa matrices diagonal and chose the following values:

$$Y_x = \begin{pmatrix} 0.43 & 0 & 0 \\ 0 & 0.1 & 0 \\ 0 & 0 & 0.43 \end{pmatrix}, \qquad Y_\nu = \begin{pmatrix} 0.001 & 0 & 0 \\ 0 & 0.00025 & 0 \\ 0 & 0 & 0.0001 \end{pmatrix}, \tag{4.1}$$

It is assumed that the four possible combinations of the signs of μ and μ' provide physically equivalent mass spectra which are slightly shifted by other parameters. Thus, in this study both signs were chosen to be positive, i.e. $\operatorname{sgn}\mu = \operatorname{sgn}\mu' = +1$. Further, the Z' mass was set to be 2000 GeV. Then we used the remaining parameters to find promising points in the parameter space.

In the first place, a parameter set satisfying the mass condition (3.12) was searched for. Due to the fixed input $M_{Z'} = 2000\,\text{GeV}$ we looked for sneutrino masses of less than 1000 GeV, chargino masses of 200 to 300 GeV and the lightest neutralino being the LSP with a mass of approximately 100 GeV. It was hard to obtain low enough masses of the sneutrinos and charginos while keeping the Higgs mass higher than 124 GeV. Moreover, it posed difficulties to keep a mass difference between the charginos and the neutralinos.

The main challenge while exploring the parameter space was that the parameters are coupled to each other. For every point in the parameter space the dependency of the masses on one certain parameter differs. Still, some general relationships were be found. In the following, the parameters shall be discussed only in view of the masses relevant in the chargino chain. However, saying that one parameter influences a certain mass does not exclude the fact that it also influences other masses. Table 9 displays which parameters have a considerable impact on a particular particle mass.

After a region in the parameter space meeting the mass conditions was found,

branching ratios were also taken into account. The desired set should have high branching ratios for decay modes to the chargino chain and small branching ratios for other processes. A first benchmark point in the parameter space is given by the input parameters shown in Table 10 producing the mass spectrum given in Table 11. This point will be refered to as Set 1.0 and provide a basis for further analysis.

Looking at the scalar und pseudoscalar sneutrino masses in Table 11, we observe the following:

$$\begin{aligned} m(\tilde{\nu}_4^S) &= m(\tilde{\nu}_2^P) \\ m(\tilde{\nu}_5^S) &= m(\tilde{\nu}_3^P) \\ m(\tilde{\nu}_6^S) &= m(\tilde{\nu}_4^P) \end{aligned}$$

These are the mass eigenstates $\tilde{\nu}_L$ as we know that no mass splitting occurs between the left-handed sneutrinos.

Parameter	Value	
$M_{Z'}$	2000	GeV
$\operatorname{sgn}\mu$	1	
$\operatorname{sgn}\mu'$	1	
$\tan\beta$	10.0001	
$\tan\beta'$	1.30	
M_B	600	GeV
M_W	480	GeV
M_G	3000	GeV
$M_{B'}$	100	GeV
A_0	800	GeV
m_Q	3200	GeV
m_L	1600	GeV
$m_{\tilde{\nu}}$	400	GeV
m_{H_u}	1100	GeV
m_{H_d}	1520	GeV
m_η	1100	GeV
$m_{\bar{\eta}}$	1520	GeV

Table 10: Parameter Set 1.0

4.3 Z' Mass Dependance of the Benchmark Point

For this thesis, we studied $Z' \to e^+e^-$ processes in the regime of Set 1.0. Figure 3 shows a scan of the parameter space in terms of $M_{Z'}$ and $\tan\beta'$ around the benchmark point highlighted in red. White space displays the regions where no

Particle		Mass [GeV]
Z' boson	Z'	2000.00
Scalar sneutrinos	$\tilde{\nu}_1^S$	424.11
	$\tilde{\nu}_2^S$	1473.73
	$\tilde{\nu}_3^S$	1473.73
	$\tilde{\nu}_4^S$	1609.10
	$\tilde{\nu}_5^S$	1616.06
	$\tilde{\nu}_6^S$	1616.08
Pseudoscalar sneutrinos	$\tilde{\nu}_1^P$	441.63
	$\tilde{\nu}_2^P$	1609.10
	$\tilde{\nu}_3^P$	1616.06
	$\tilde{\nu}_4^P$	1616.08
	$\tilde{\nu}_5^P$	1861.97
	$\tilde{\nu}_6^P$	1861.97
Charginos	$\chi_1^\pm$	339.61
	$\chi_2^\pm$	4045.78
Neutralinos	χ_1^0	248.92
	χ_2^0	339.43
	χ_3^0	715.40
	χ_4^0	1669.91
	χ_5^0	2419.41
	χ_6^0	4044.95
	χ_7^0	4045.44
Higgs bosons	h^0	128.48
	H^0	366.98
	h'	2835.20
	H'	4196.10
	A^0	2060.76
	A_η^0	4186.59
	H^+	4187.43

Table 11: Mass spectrum for Set 1.0

valid spectrum could be calculated by `SPheno` because scalar masses squared become negative or solutions to tadpole equations do not exist. The dark blue points are allowed points in the parameter space. The resolution is 50 GeV in terms of the Z' mass and 0.01 for $\tan\beta'$. For the original value $\tan\beta' = 1.3$ in Set 1.0, only Z' masses between 1300 GeV and 2200 GeV are valid as marked by the blue lines. Consequently, we can vary $M_{Z'}$ within this mass interval while keeping all other parameters fixed and analyse corresponding Z' resonances.

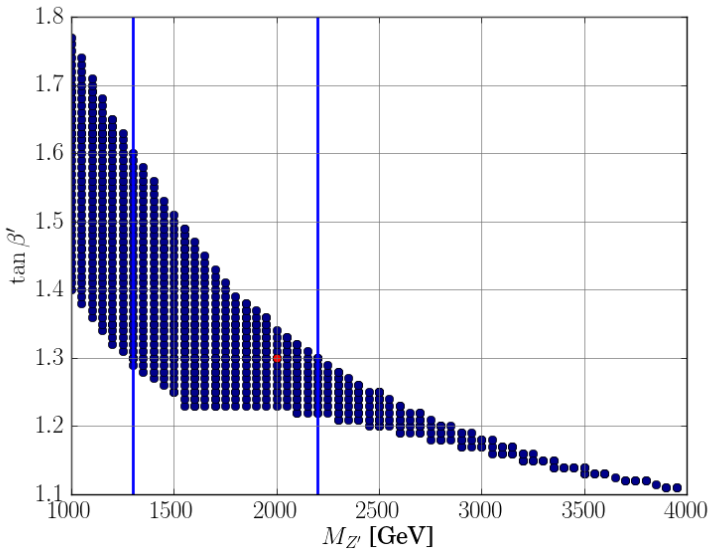

Figure 3: Study of the expanded GUT parameter space in the $M_{Z'}$-$\tan\beta'$-plane for Set 1.0. The red dot indicates the benchmark point given by Set 1.0, blue lines mark the valid Z' mass intervall for $\tan\beta' = 1.3$.

In Figure 4 the branching ratio of the Z' decaying into a dielectron pair is illustrated. The step indicates that new decaying possibilities arise with higher masses. From Figure 5 we see that it is the $Z' \to H^0 + Z$ decay that has an increasing branching fraction for Z' masses above 1800 GeV. However, within the allowed mass interval the branching ratios for the dielectron pair vary from the value at $M_{Z'} = 2000$ GeV by less than 3 %. Therefore, a constant branching fraction of 0.1 was taken for the analysis.

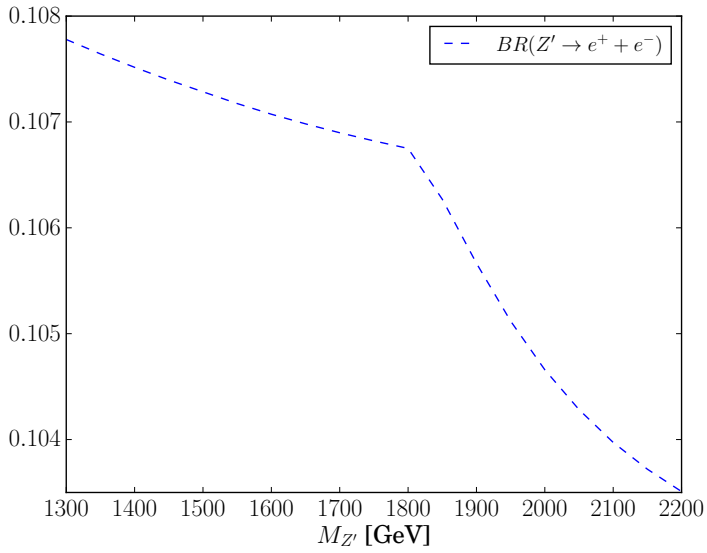

Figure 4: Branching ratio of the $Z' \to e^+e^-$ decay for Set 1.0 as a function of $M_{Z'}$. The reason for the bend is the process $Z' \to H^0 + Z$ that is possible for masses higher than 1800 GeV.

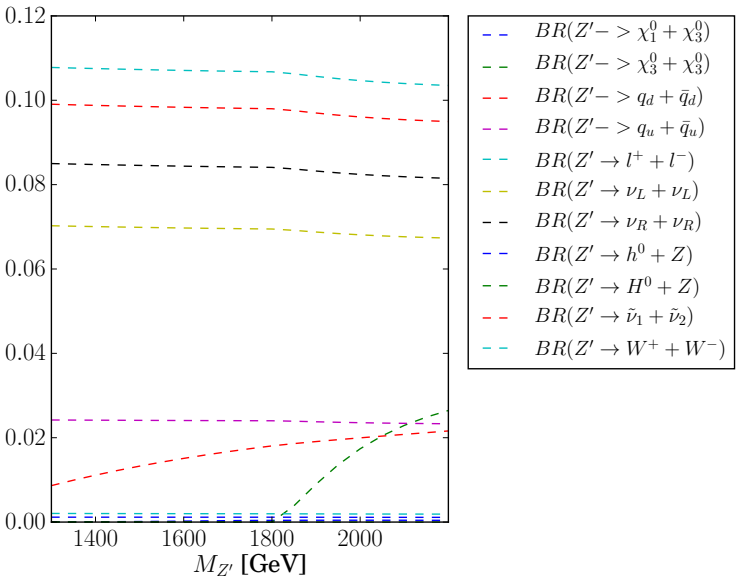

Figure 5: Branching ratios of Z' decays for Set 1.0 as a function of $M_{Z'}$. The three generations of quarks and leptons have the same branching ratios respectively. q_u are up-type quarks, q_d are down-type quarks, l denotes leptons and ν neutrinos where the index indicates left- and right-handedness. $\tilde{\nu}_i$ are the right-handed sneutrino mass eigenstates, χ_i^0 are neutralinos, and $h^0, H^0, Z, W^\pm$ are the boson mass eigenstates as in 2.2.3.

5 Event Analysis

In this section we compare decays of the Z' into dielectron final states in the BLSSM with SM dielectron events. Therefore, Z' and SM events are generated with `MadGraph` [6] and then cuts are applied with `CheckMATE` [10, 11, 12, 16, 27]. We find the 95 % confidence level for excluding the Z' as signal phenomenon using the CL_s method. Finally, the exclusion limits of the Z' mass are calculated.

5.1 Dielectron Event Generation: Simulation of Signal and Background

Both event generation and calculation of cross sections were done with `MadGraph`. The software package `MadGraph` is an event generator that produces sets of particles with given momenta and quantum numbers according to their cross sections. For this study the BLSSM was implemented in `MadGraph` and the `SPheno` output was modified to become an parameter input file for `MadGraph` [5].

In the study of proton-proton collisions it is important to keep in mind that protons are composite particles made up of quarks and gluons, also refered to as partons. Thus, the scattering of two protons results in the collision of partons. The probability of finding a certain parton in the proton is given by particle distribution functions (PDFs). `MadGraph` uses experimentally determined PDFs to calculate the scattering correctly. Many of the outgoing particles of a high energy scattering are unstable particles that decay before they reach the detector. If these particles are coloured, they will radiate gluons and quarks and eventually build more massive final state hadrons. These processes are implemented in parton shower and hadronisation routines using the software package `Pythia` [24].

Our signal events are $p + p \to Z' \to e^+e^-$ processes in the regime of Set 1.0 in the BLSSM. These were generated for different Z' masses. As background we considered all proton-proton collisions that lead to dielectron events in the SM, that is the generation of $p + p \to e^+e^-$ in the SM.

In order to estimate the cross section error, every process was generated with two different PDFs, with the default PDF `nn23lo1` and for comparism also with `cteq6l1`. We used the default renormalization and factorization scale of `MadGraph`. That means for signal events the scale was set to $M_{Z'}^2 + p_T^2$ with p_T being the transverse momentum and for background events to the invariant mass squared of the dielectron pair [1]. This scale was further varied by a factor. Event generation for both PDFs each with the scalefactors 0.5, 1.0, and 2.0 lead to six cross sections. Then the minimal and the maximal value were used to obtain the cross section:

$$\sigma = \frac{1}{2}(\sigma_{\max} + \sigma_{\min}) \tag{5.1}$$

$$\Delta\sigma = \frac{1}{2}(\sigma_{\max} - \sigma_{\min}) \tag{5.2}$$

We generated 10 000 events for both signal and background using standard `MadGraph` cuts where we demanded a lepton transverse momentum of at least

20 GeV. The center-of-mass energy was chosen to be 13 TeV. First, the valid parameter region of Z' masses between 1300 GeV and 2200 GeV was investigated in steps of 50 GeV. Here we added an invariant dilepton mass cut of 1000 GeV to ensure that we obtain enough background events.

In a second step also higher mass resonances were looked at. Because for Set 1.0 Z' masses above 2200 GeV are not allowed, we manually changed the mass parameter in the input file for `MadGraph`. Accordingly, also the width of the Z' had to be increased. Therefore, the width calculated by `SPheno` was fitted linearly such that the width for higher Z' masses could be calculated. Figure 6 shows the behaviour of the Z' width in the regime of Set 1.0. Moreover, the invariant mass cut of the dielectron pair was adapted. For the analysis of the mass range from 2500 GeV to 4500 GeV we demanded a dilepton mass higher than 2300 GeV and for the mass range from 4500 GeV to 6000 GeV we demanded more than 4300 GeV.

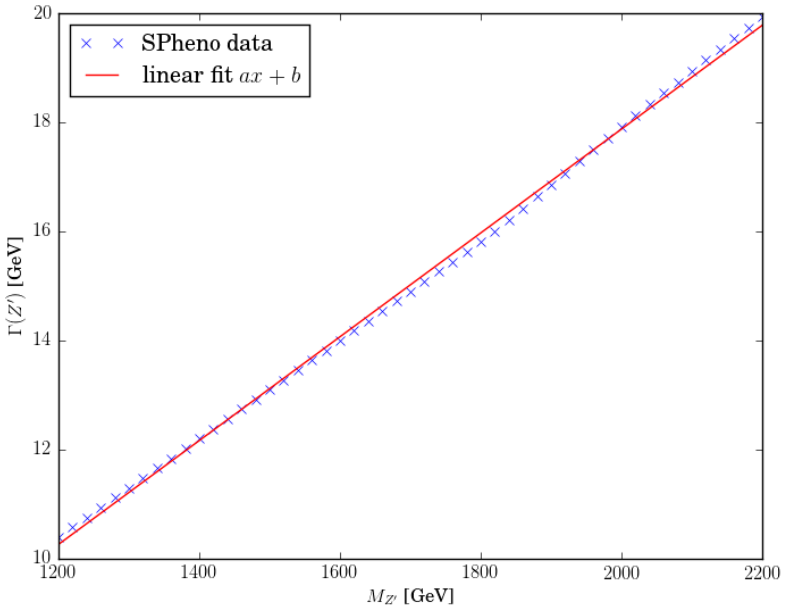

Figure 6: Width of the Z' with linear fit $a = 0.009515$ and $b = -1.153897$

5.2 Event selection

`CheckMATE` was used to create histograms and count the dielectron events in a certain mass interval. In order to accurately model the LHC reach, `CheckMATE` uses `Delphes` for the detector simulation.

We will first consider histograms in terms of the dielectron invariant mass. Figure 7 shows histograms of the SM events, where different dielectron mass cuts have been applied at the Monte-Carlo generator level. In Figure 8 there are histograms for different $M_{Z'}$ input values in the BLSSM. The plots clearly display the resonance of the Z' boson. Also the increasing width of the peak for higher Z' masses can be seen.

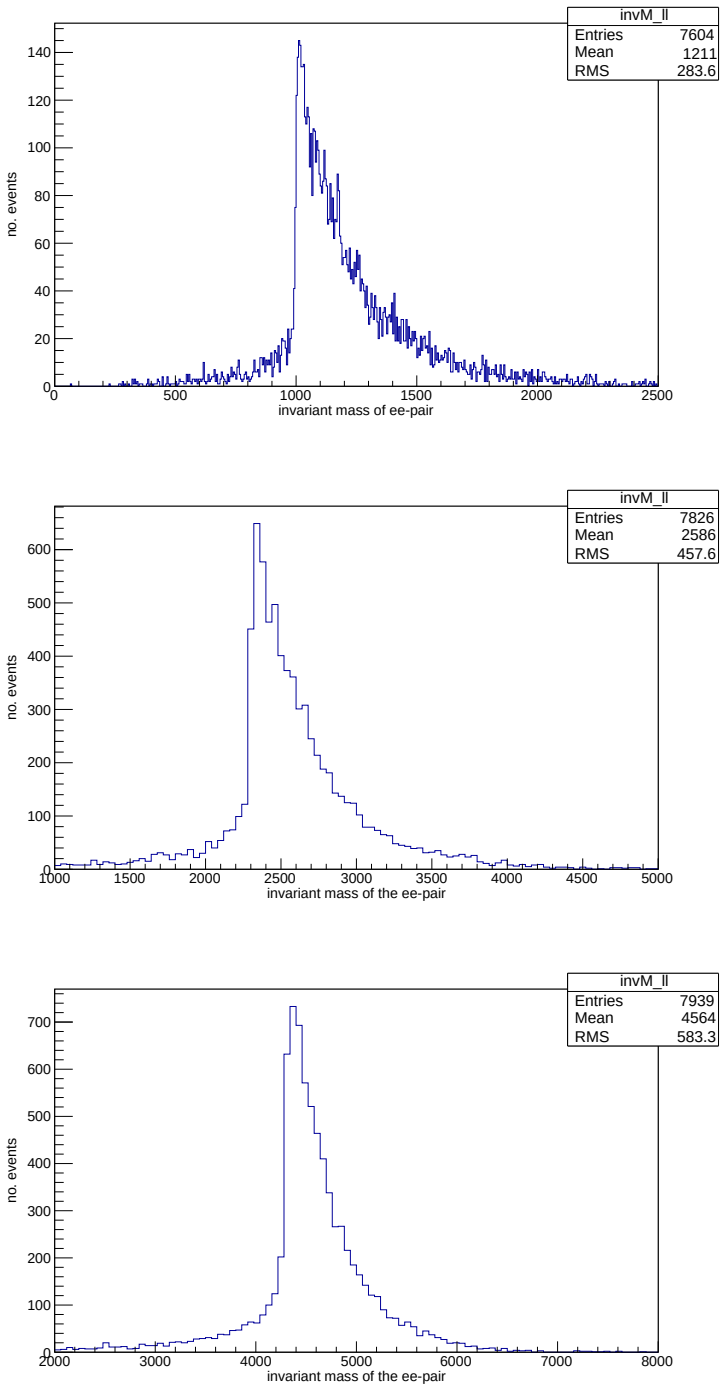

Figure 7: Histograms of the invariant mass of the dielectron pair for SM processes $p + p \to e^+e^-$. At the Monte-Carlo generator level the transverse momentum cut is $p_T > 20\,\text{GeV}$ and the dilepton mass cuts are $m_{e\bar{e}} > 1000\,\text{GeV}$ (top), $m_{e\bar{e}} > 2300\,\text{GeV}$ (middle), and $m_{e\bar{e}} > 4300\,\text{GeV}$ (bottom)

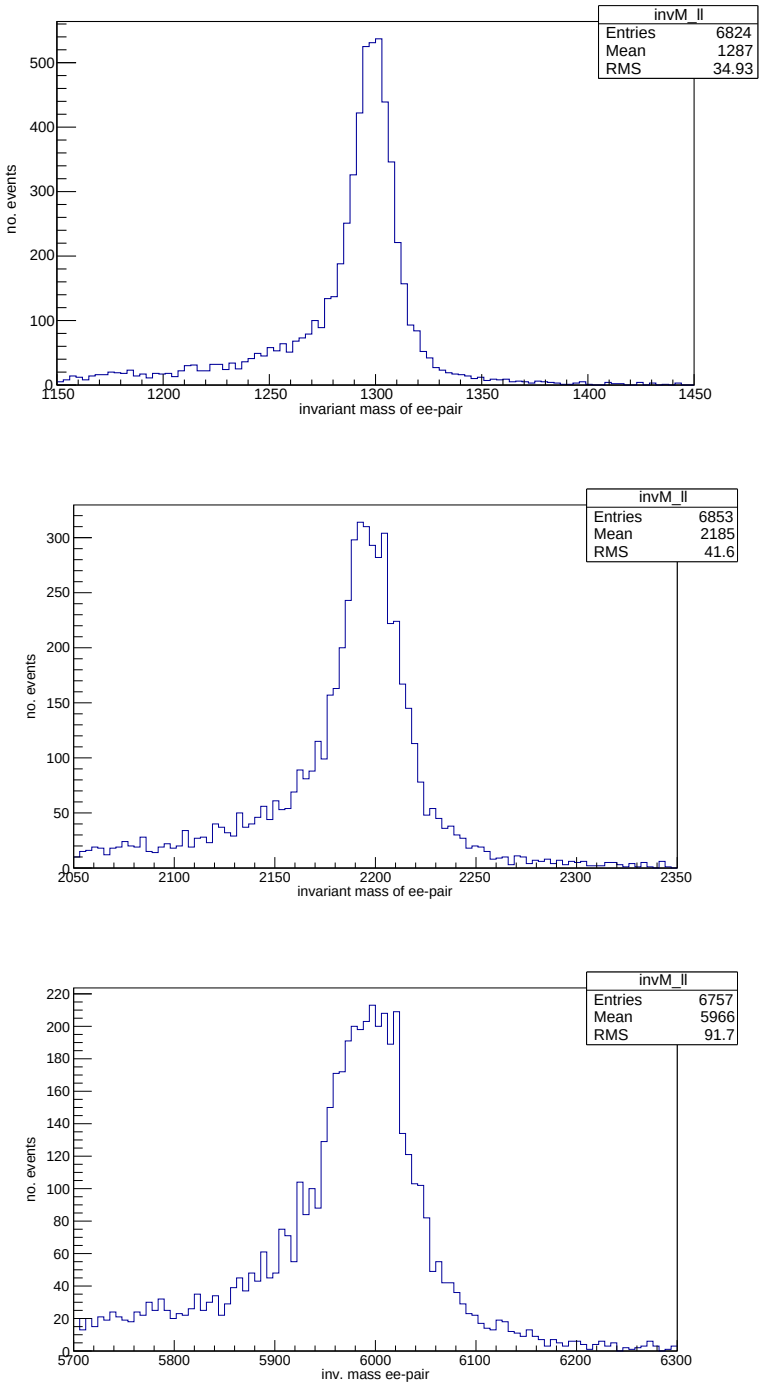

Figure 8: Histograms of the invariant mass of the dielectron pair for $p + p \to Z' \to e^+e^-$ processes in the BLSSM with $m_{Z'} = 1300\,\text{GeV}$ (top), $m_{Z'} = 2200\,\text{GeV}$ (middle), and $m_{Z'} = 6000\,\text{GeV}$ (bottom). At the Monte-Carlo generator level the transverse momentum cut is $p_T > 20\,\text{GeV}$ and the dilepton mass cuts are $m_{e\bar{e}} > 1000\,\text{GeV}$ (top and middle) and $m_{e\bar{e}} > 4300\,\text{GeV}$ (bottom)

For allowed $M_{Z'}$ values the signal area was chosen to be the interval from $(M_{Z'} - 50\,\text{GeV})$ to $(M_{Z'} + 50\,\text{GeV})$. Figure 8 shows that this interval is wide enough to cover the whole Z' peak also for the maximal Z' mass of 2200 GeV in Set 1.0. When signal and background were analysed for higher Z' masses, the increased width required bigger signal regions. For the intervall from 5000 GeV to 6000 GeV a signal region of $M_{Z'} \pm 100\,\text{GeV}$ was chosen after considering the width at $M_{Z'} = 6000\,\text{GeV}$ shown in Figure 8.

A `CheckMATE` analysis was then carried out for signal and background seperately to determine the number of oppositly charged dielectron events in the signal area. This allows the relative number of events to be obtained, i.e. number of events in the signal region n divided by the total number of generated events N. Since the integrated luminosity $\mathcal{L}$ is the number of events per cross section, the product $\mathcal{L} \cdot \sigma$ describes the number of events. Then the normalized number of events can be expressed as follows:

$$n_{\text{norm}} = \mathcal{L}\sigma\frac{n}{N} \tag{5.3}$$

For large n the standard deviation is given by the square root of n. Since the relative cross section error is around 10 %, we will neglect the error of the luminosity.

$$\Delta n = \sqrt{n} \tag{5.4}$$

$$\Rightarrow \frac{\Delta n_{\text{norm}}}{n_{\text{norm}}} = \sqrt{\left(\frac{\Delta n}{n}\right)^2 + \left(\frac{\Delta\sigma}{\sigma}\right)^2} \tag{5.5}$$

$$\Delta n_{\text{norm}} = \sqrt{\left(\frac{1}{n}\right) + \left(\frac{\Delta\sigma}{\sigma}\right)^2}\, n_{\text{norm}} \tag{5.6}$$

In the following, the number of events will always refer to the normalized number of events. Our analysis will be carried out for luminosities of $20\,\text{fb}^{-1}$, $100\,\text{fb}^{-1}$, and $3000\,\text{fb}^{-1}$.

5.3 The Significance of a Signal and CL$_s$ Limits

The aim of searching experiments in particle physics is to detect predicted phenomena. Then there are two hypothesis, either the phenomenon exists or not. Thereby "significance" denotes the probability α to reject a true hypothesis. Here, the significance of a signal in the presence of background processes shall be analysed. Let s be the number of signal events, i.e. the events indicating a new phenomenon, and b the number of background events. If the observed number of events n_{obs} is significantly greater than b, the background-hypothesis can be rejected and a discovery claimed; if n_{obs} is significantly less than $s + b$, the signal-plus-background-hypothesis can be rejected and thus the phenomenon can be excluded. Depending on the value of n_{obs} one would either state that the phenomenon exists or not. This means n_{obs} follows a

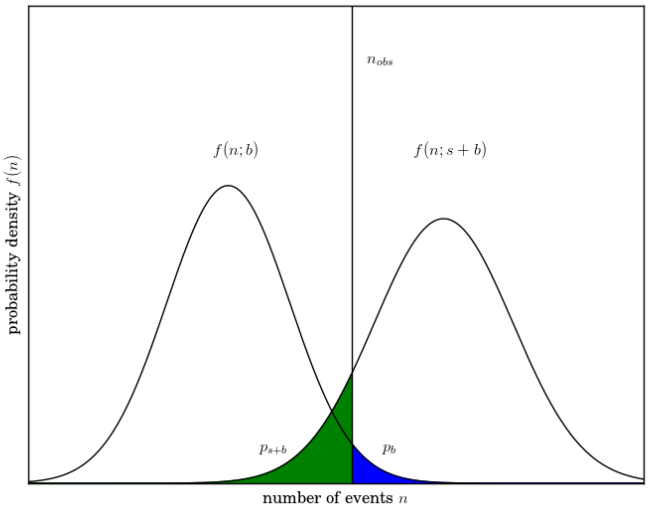

Figure 9: Probability distribution functions and p-values for a given number of observed events n_{obs}. The p-value for probability density of the signal-plus-background-hypothesis $f(n; s + b)$ is marked in green, and of the background-hypothesis $f(n; b)$ in blue.

binomial distribution. For a small probability of one hypothesis and a large number of trials the binomial distribution is well approximated by a Poisson distribution.

If λ is the average number of events in a given interval, then the probability to count n events in this interval is according to the Poisson distribution

$$f(n;\lambda) = \frac{e^{-\lambda}\lambda^n}{n!} \tag{5.7}$$

The variance squared of a Poisson distribution is equal to the mean value.

$$\sigma = \sqrt{\lambda} \tag{5.8}$$

For quantitative statements regarding some hypothesis, so-called p-values are calculated. Here it is assumed that the signal-plus-background distribution is shifted to the right, i.e. $s+b > b$ as shown in Figure 9. Then the p-value of the background-only-hypothesis is defined as the probability to find a value n greater or equal to n_{obs} assuming that there is only background:

$$p_b = P(n \geq n_{obs}; b) = \int_{n_{obs}}^{+\infty} f(n;b) \tag{5.9}$$

For the signal-plus-background distribution the p-value describes the probability to find $n \leq n_{obs}$ under the assumption that the signal phenomenon exists:

$$p_{s+b} = P(n \leq n_{obs}; s+b) = \int_{-\infty}^{n_{obs}} f(n;s+b) \tag{5.10}$$

This is the probability to reject a signal-plus-background-hypothesis although it is true. One usually demands a confidence level of 95 %, i.e. $p_{s+b} = \alpha < 5\,\%$, such that the probability to falsely exclude an existing phenomenon is less than 5 %. But if $s \ll b$, which means the distributions of $s + b$ and b are very close to each other, the sensitivity of this values is much weaker than if $s + b$ is significantly bigger than b. To take this into accound, in the CL_s method the value used to exclude a signal is the ratio of the aforementioned p-values:

$$\mathrm{CL}_s \equiv \frac{p_{s+b}}{1 - p_b} \tag{5.11}$$

For $f(n; s+b)$ and $f(n; b)$ well separated, in a signal-plus-background measurement $1 - p_b$ will be slightly less than 1, such that CL_s is dominated by p_{s+b}. If the distributions $f(n; s+b)$ and $f(n; b)$ are close to each other, the CL_s value is increased by the $(1 - p_b)$ denominater and an exclusion due to low sensitivity is prevented. Therefore, a CL_s value greater than 5 % is used as confidence level to exclude a signal phenomenon [31, 32].

The CL_s value can be calculated by the number of observed events n_{obs}, the number of expected signal events s and the number of expected background events b. We define s_{95} to be the number of signal events such that the CL_s is 5 %. Motivated by current experimental data, we start from the premise that we only measure SM events. Hence, we assume that the number of observed events will be equal to the number of background events for the proposed search:

$$n_{\mathrm{obs}} = b \tag{5.12}$$

Then s_{95} describes the maximal upper fluctuation of the background at which a signal phenomenon is still possible. This means any model predicting $s > s_{95}$ is ruled out.

5.4 Results

The outcomes showed that for the allowed masses in Set 1.0 only a small number of background events survived whereas the number of signal events was large in comparison as can be seen in Figure 10. Since the background events are heavily suppressed compared to the signal, a plot for the number of background events is also added. One can expect from these big differences between signal and background that in this region of the parameter space the model is clearly ruled out. Proof is given in Figure 11 where the s_{95} limit is clearly smaller than the number of signal events meaning that we exclude a Z' resonance for these masses.

Although we can exclude the model by all three analyses using different luminosities, for higher luminosities the number of events increases such that the relative error is smaller. The errors were estimated by the statistical error of the number of events and the cross section error according to (5.6). For a luminosity of $20\,\mathrm{fb}^{-1}$ there is still an statistical error of almost 20 % on signal events at 2000 GeV and

the number of background events is much too small to use the $\sqrt{n}$ approximation for proper errors. In contrast, at luminosities of $100\,\mathrm{fb}^{-1}$ and $3000\,\mathrm{fb}^{-1}$ the errors on the signal are less than 8 % and 1.5 % respectively. While the maximal error on the number of background events is less than 12.5 % for $3000\,\mathrm{fb}^{-1}$, for $100\,\mathrm{fb}^{-1}$ it is almost 70 %.

At higher mass scales the background is effectively zero since the number of events becomes very small. In Figure 13 the number of signal events and background events are displayed. When calculating the exclusion limits for very small numbers of observed events, the boundary s_{95} becomes asymptotic with a value of approximately 2.9 as can be seen in Figure 12. Thus, we are looking for the mass $M_{Z'}$ when less than three signal events are produced. This is essentially determined by the cross section of the $Z' \to e^+e^-$ process. The exponential decrease of the cross section is displayed in Figure 15.

The critical regions for the exclusion are shown in Figure 14, where the number of signal events becomes smaller than the s_{95} limit. We use the error of the signal events to estimate the error of the exclusion limit. Extrapolation and fitting of the plots lead the intersection points in Table 12.

$\mathcal{L}$	$M_{95} - 2\sigma$	$M_{95} - \sigma$	M_{95}	$M_{95} + \sigma$	$M_{95} + 2\sigma$
$20\,\mathrm{fb}^{-1}$	3102 GeV	3184 GeV	3243 GeV	3291 GeV	3340 GeV
$100\,\mathrm{fb}^{-1}$	3800 GeV	3872 GeV	3934 GeV	3991 GeV	4048 GeV
$3000\,\mathrm{fb}^{-1}$	5128 GeV	5300 GeV	5445 GeV	5550 GeV	5655 GeV

Table 12: Intersection points of signal, signal $\pm\sigma$, and signal $\pm 2\sigma$ with s_{95}

Taking the average of the upper and lower 1σ error, we obtain the following results:

$$\begin{aligned} M_{95} &= (3243 \pm 54)\,\mathrm{GeV} && \text{for } \mathcal{L} = 20\,\mathrm{fb}^{-1} \\ M_{95} &= (3934 \pm 60)\,\mathrm{GeV} && \text{for } \mathcal{L} = 100\,\mathrm{fb}^{-1} \\ M_{95} &= (5445 \pm 125)\,\mathrm{GeV} && \text{for } \mathcal{L} = 3000\,\mathrm{fb}^{-1} \end{aligned} \tag{5.13}$$

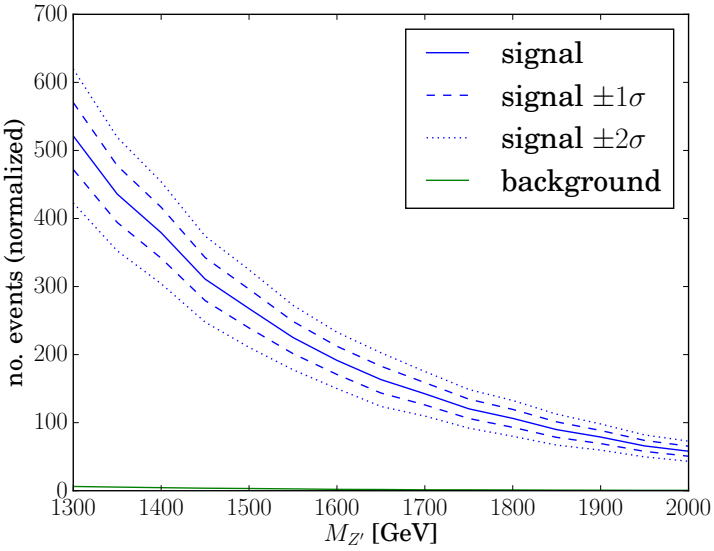

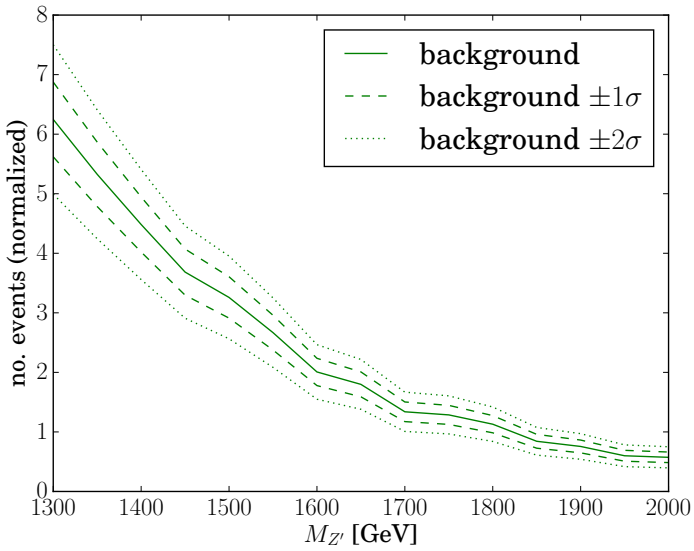

Figure 10: Normalized number of signal and background events in the signal region for a luminosity of $20\,\mathrm{fb}^{-1}$. The plots for $100\,\mathrm{fb}^{-1}$ and $3000\,\mathrm{fb}^{-1}$ have the same behavior for a larger number of events.

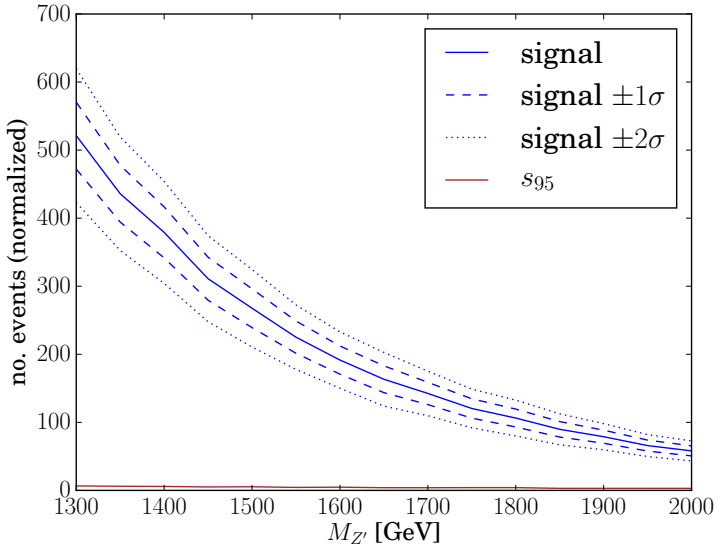

Figure 11: Normalized number of signal events and the s_{95} limit on signal events for a luminosity of $20\,\mathrm{fb}^{-1}$. The plots for $100\,\mathrm{fb}^{-1}$ and $3000\,\mathrm{fb}^{-1}$ have the same behavior for a larger number of events.

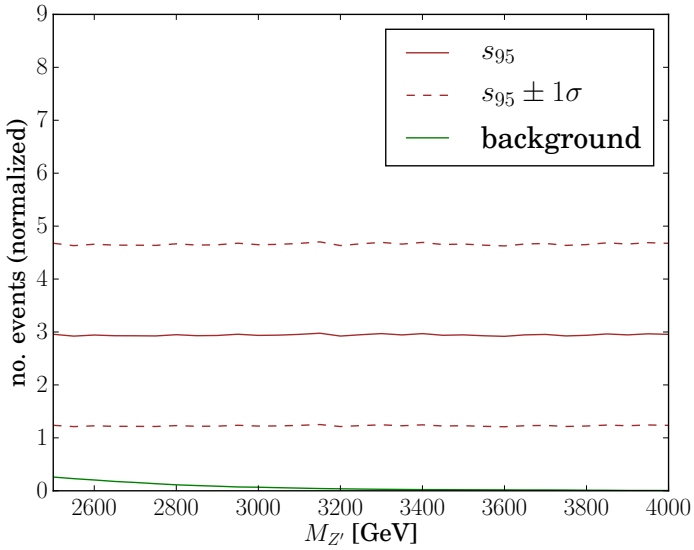

Figure 12: The s_{95} limit as a function of the number of background events for a luminosity of $20\,\mathrm{fb}^{-1}$. Due to the small number of background events s_{95} behaves asymptotically. The same applies to $100\,\mathrm{fb}^{-1}$ and $3000\,\mathrm{fb}^{-1}$.

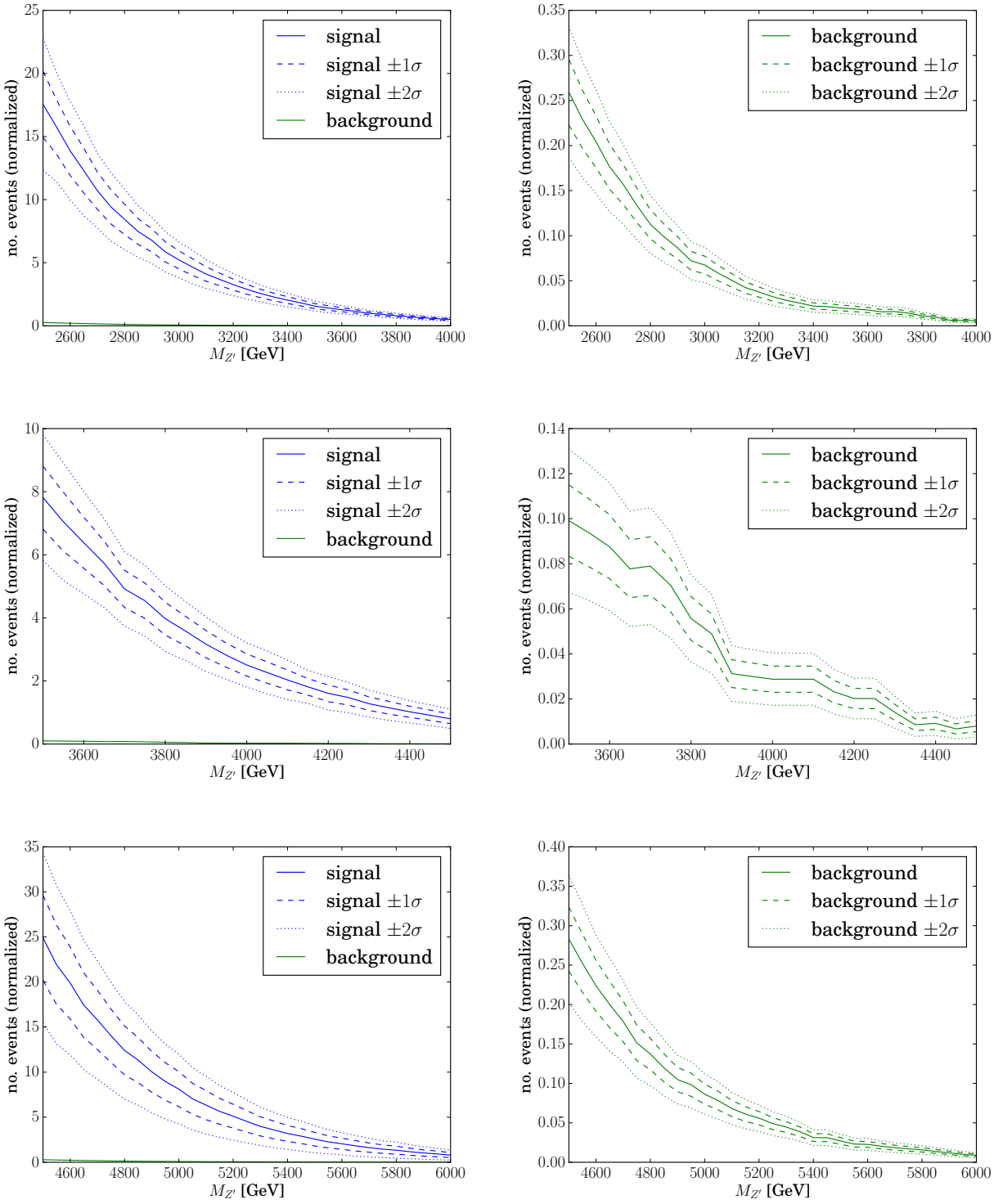

Figure 13: Normalized number of signal and background events in the signal region for luminosities of $20\,\mathrm{fb}^{-1}$ (top row), $100\,\mathrm{fb}^{-1}$ (middle row) and $3000\,\mathrm{fb}^{-1}$ (bottom row)

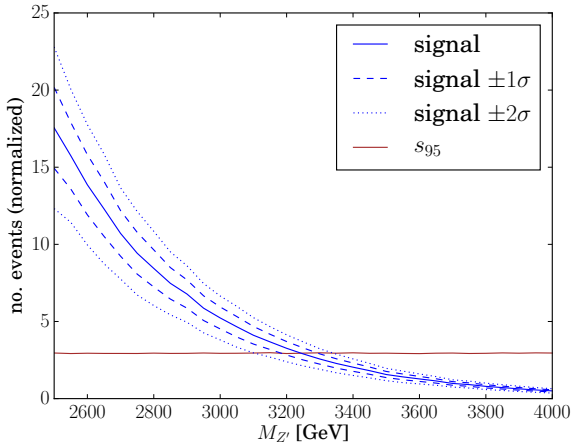

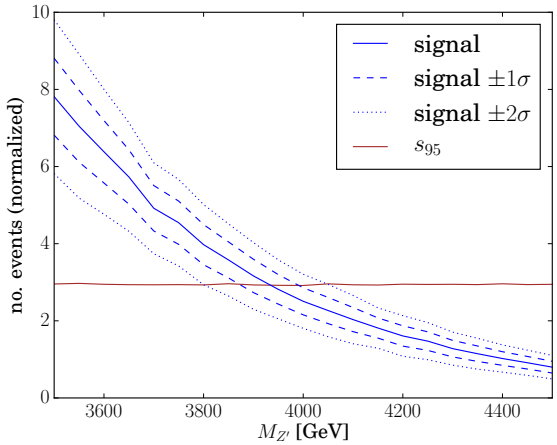

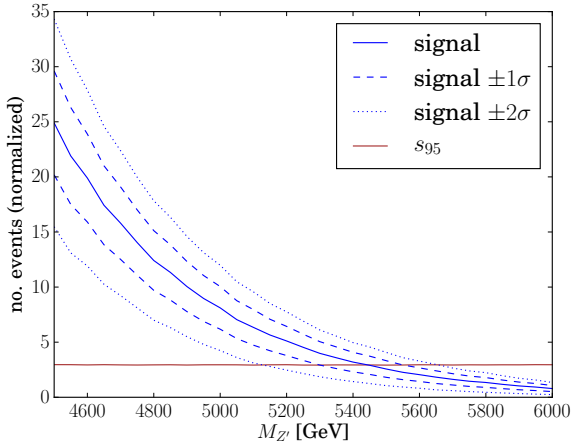

Figure 14: The number of signal events and the 95 % exclusion limit

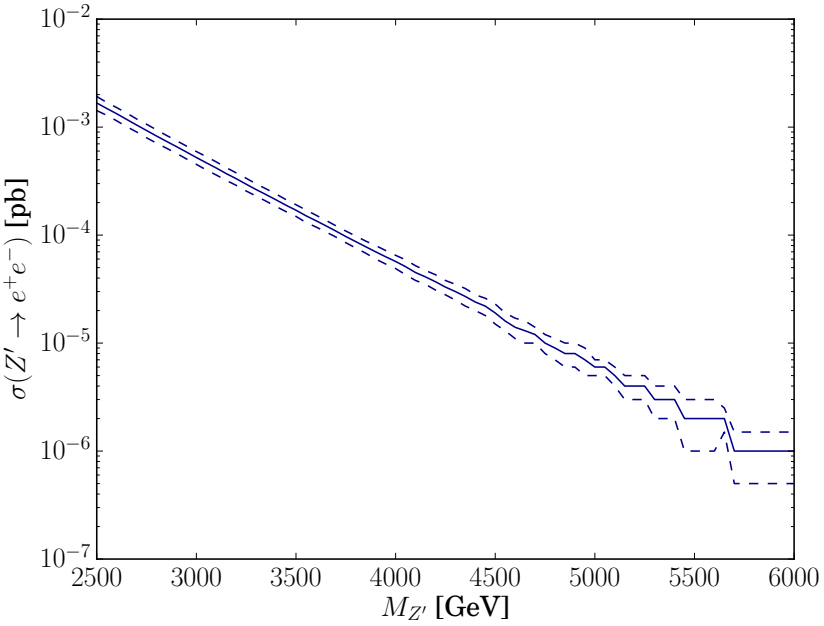

Figure 15: Cross section of signal events in a logarithmic scale

6 Conclusion

The aim of this thesis was to investigate Z' resonances decaying to a dielectron final state for a parameter set in the BLSSM that was intended to examine sneutrino-antisneutrino oscillations. In the given regime it was found that the model can be excluded for valid Z' masses in the parameter space if no signal is detected at the LHC. An extrapolation to higher masses delivered possible exclusion limits on the Z' mass. We found that Z' resonances can be excluded below 3.2 TeV for a luminosity of $20\,\text{fb}^{-1}$, below 3.9 TeV for $100\,\text{fb}^{-1}$, and below 5.4 TeV for $3000\,\text{fb}^{-1}$.

This can be compared to current searches for high-mass resonances decaying to dilepton final states at the ATLAS detector at the Large Hadron Collider. The data recorded in proton-proton collisions at a center-of-mass energy of 8 TeV and an integrated luminosity of $20.3\,\text{fb}^{-1}$ in the dielectron channel in 2012 lead to an exclusion of a Z' mass resonance below 2.22 TeV at 95% confidence level [3]. Therefore, according to our results, the 13 TeV run is expected to significantly improve the current searches.

References

[1] URL: https://cp3.irmp.ucl.ac.be/projects/madgraph/wiki/FAQ-General-13?format=pdfarticle (visited on 02/23/2015).

[2] Georges Aad et al. "Observation of a new particle in the search for the Standard Model Higgs boson with the ATLAS detector at the LHC". In: *Phys.Lett.* B716 (2012), pp. 1–29. DOI: 10.1016/j.physletb.2012.08.020. arXiv: 1207.7214 [hep-ex].

[3] Georges Aad et al. "Search for high-mass dilepton resonances in pp collisions at $\sqrt{s} = 8$â â TeV with the ATLAS detector". In: *Phys.Rev.* D90.5 (2014), p. 052005. DOI: 10.1103/PhysRevD.90.052005. arXiv: 1405.4123 [hep-ex].

[4] W. Abdallah, S. Khalil, and S. Moretti. "Double Higgs peak in the minimal SUSY B-L model". In: *Phys.Rev.* D91.1 (2015), p. 014001. DOI: 10.1103/PhysRevD.91.014001. arXiv: 1409.7837 [hep-ph].

[5] Johan Alwall et al. "MadGraph 5 : Going Beyond". In: *JHEP* 1106 (2011), p. 128. DOI: 10.1007/JHEP06(2011)128. arXiv: 1106.0522 [hep-ph].

[6] J. Alwall et al. "The automated computation of tree-level and next-to-leading order differential cross sections, and their matching to parton shower simulations". In: *JHEP* 1407 (2014), p. 079. DOI: 10.1007/-JHEP07(2014)079. arXiv: 1405.0301 [hep-ph].

[7] Vernon Barger and Roger Phillips. *Collider Physics*. Ed. by David Pines. Addison-Wesley Publishing Company, 1987.

[8] Lorenzo Basso, Stefano Moretti, and Giovanni Marco Pruna. "Phenomenology of the minimal $B-L$ extension of the Standard Model: the Higgs sector". In: *Phys.Rev.* D83 (2011), p. 055014. DOI: 10.1103/PhysRevD.83.055014. arXiv: 1011.2612 [hep-ph].

[9] Alessandro Bettini. *Introduction to elementary particle physics*. Cambridge University Press, 2014.

[10] Matteo Cacciari and Gavin P. Salam. "Dispelling the N^3 myth for the k_t jet-finder". In: *Phys.Lett.* B641 (2006), pp. 57–61. DOI: 10.1016/j.physletb.2006.08.037. arXiv: hep-ph/0512210 [hep-ph].

[11] Matteo Cacciari, Gavin P. Salam, and Gregory Soyez. "FastJet User Manual". In: *Eur.Phys.J.* C72 (2012), p. 1896. DOI: 10.1140/epjc/s10052-012-1896-2. arXiv: 1111.6097 [hep-ph].

[12] Matteo Cacciari, Gavin P. Salam, and Gregory Soyez. "The Anti-k(t) jet clustering algorithm". In: *JHEP* 0804 (2008), p. 063. DOI: 10.1088/1126-6708/2008/04/063. arXiv: 0802.1189 [hep-ph].

[13] D.J.H. Chung et al. "The Soft supersymmetry breaking Lagrangian: Theory and applications". In: *Phys.Rept.* 407 (2005), pp. 1–203. DOI: 10.1016/j.physrep.2004.08.032. arXiv: hep-ph/0312378 [hep-ph].

[14] Wikimedia Commons. URL: http://commons.wikimedia.org/wiki/File:Standard_Model_of_Elementary_Particles.svg (visited on 04/30/2014).

[15] A. Elsayed et al. "Right-handed sneutrino-antisneutrino oscillations in a TeV scale Supersymmetric B-L model". In: *Phys.Rev.* D87.5 (2013), p. 053010. DOI: 10.1103/PhysRevD.87.053010. arXiv: 1211.0644 [hep-ph].

[16] J. de Favereau et al. "DELPHES 3, A modular framework for fast simulation of a generic collider experiment". In: *JHEP* 1402 (2014), p. 057. DOI: 10.1007/JHEP02(2014)057. arXiv: 1307.6346 [hep-ex].

[17] Martin Fluder. "The Minimal Supersymmetric Standard Model". 2010. URL: http://www.itp.phys.ethz.ch/education/fs10/susy.

[18] Francis Halzen and Alan D. Martin. *QUARKS AND LEPTONS: An Introductory Course in Modern Particle Physics*. John Wiley & Sons, Inc., 1984. ISBN: 0-471-88741-2.

[19] Roger H.K. Kadala. *Topics in supersymmetry phenomenology at the Large Hadron Collider*. 2012. arXiv: 1205.1267 [hep-ph].

[20] Shaaban Khalil. "Low scale $B - L$ extension of the Standard Model at the LHC". In: *J.Phys.* G35 (2008), p. 055001. DOI: 10.1088/0954-3899/35/5/055001. arXiv: hep-ph/0611205 [hep-ph].

[21] Manuel Krauß. "LHC Phenomenology of a Z' decaying into supersymmetric particles". URL: http://www.physik.uni-wuerzburg.de/fileadmin/11030200/Master_Arbeiten/krauss-manuel_master.pdf.

[22] Stephen P. Martin. "A Supersymmetry primer". In: *Adv.Ser.Direct.High Energy Phys.* 21 (2010), pp. 1–153. DOI: 10.1142/9789814307505_0001. arXiv: hep-ph/9709356 [hep-ph].

[23] Ben O'Leary, Werner Porod, and Florian Staub. "Mass spectrum of the minimal SUSY $B - L$ model". In: *JHEP* 1205 (2012), p. 042. DOI: 10.1007/JHEP05(2012)042. arXiv: 1112.4600 [hep-ph].

[24] Maxim Perelstein. *Introduction to Collider Physics*. 2010. arXiv: 1002.0274 [hep-ph].

[25] Werner Porod. "SPheno, a program for calculating supersymmetric spectra, SUSY particle decays and SUSY particle production at e^+e^- colliders". In: *Computer physics communications* 153.2 (2003), pp. 275–315.

[26] Werner Porod and Florian Staub. "SPheno 3.1: Extensions including flavour, CP-phases and models beyond the MSSM". In: *Computer Physics Communications* 183.11 (2012), pp. 2458–2469.

[27] Alexander L. Read. "Presentation of search results: The CL(s) technique". In: *J.Phys.* G28 (2002), pp. 2693–2704. DOI: 10.1088/0954-3899/28/10/313.

[28] Florian Staub. "Automatic calculation of supersymmetric renormalization group equations and loop corrections". In: *JHEP* 182.3 (2011), pp. 808–833. arXiv: 1002.0840[hep-ph].

[29] Florian Staub. "Linking SARAH and MadGraph using the UFO format". In: *JHEP* (2012). arXiv: 1207.0906[hep-ph].

[30] Florian Staub. "SARAH". In: *JHEP* (2008). arXiv: 0806.0538[hep-ph].

[31] *The CLs method: information for conference speakers*. URL: http://www.pp.rhul.ac.uk/~cowan/atlas/CLsInfo.ps.

[32] J. Wagner. "Physikalisches Praktikum I für Studierende der Physik, Geowissenschaften und Mathematik". URL: https://www.physi.uni-heidelberg.de/Einrichtungen/AP/anleitungen/pap.php.

Acknowledgement

I want to thank Tilman Plehn for giving me the opportunity to work on this project and Jamie Tattersall for his guidance. I also have to thank Mike Bisset that he provided me an insight to particle phenomenology and introduced me to this project. Many thanks to Ran Lu for his support in terms of software. Also thanks to the group for answering all kinds of questions.

Erklärung

Ich versichere, dass ich diese Arbeit selbstständig verfasst und keine anderen als die angegebenen Quellen und Hilfsmittel benutzt habe.

Heidelberg, den 24.2.2015,

Linda Shen